2Aminopurine non-radiative decay and emission in aqueous solution: A theoretical study

6 AUTHORS, INCLUDING:

Valdemir Ludwig
University of São Paulo
17 PUBLICATIONS 255 CITATIONS

SEE PROFILE

Marcos Serrou Amaral
Universidade Federal de Mato Grosso do Sul
17 PUBLICATIONS 69 CITATIONS

SEE PROFILE

Antonio Carlos Borin
University of São Paulo
75 PUBLICATIONS 1,436 CITATIONS

SEE PROFILE

Sylvio Canuto
University of São Paulo
249 PUBLICATIONS 3,239 CITATIONS

SEE PROFILE

2-Aminopurine non-radiative decay and emission in aqueous solution: A theoretical study

Valdemir Ludwig [a,*], Marcos Serrou do Amaral [a], Zélia M. da Costa [b], Antonio Carlos Borin [c], Sylvio Canuto [d], Luis Serrano-Andrés [e]

[a] Departamento de Física, CCET, Universidade Federal do Mato Grosso do Sul CP 549, CEP 79070-900 Campo Grande, MS, Brazil
[b] Departamento de Física, Universidade Federal de Juiz de Fora, 36036-900 Juiz de Fora, MG, Brazil
[c] Instituto de Química, Universidade de São Paulo, Av. Prof. Lineu Prestes 748, 05508-900 São Paulo, SP, Brazil
[d] Instituto de Física, Universidade de São Paulo, CP 66318, 05315-970 São Paulo, SP, Brazil
[e] Instituto de Ciencia Molecular, Universitat de València, Apartado 22085, ES-46071 Valencia, Spain

ARTICLE INFO

ABSTRACT

The minimum energy path along the lowest-lying $\pi\pi^*$ excited state of 2-aminopurine was calculated to elucidate the mechanisms of radiationless decay and emission in water. The sequential Monte Carlo quantum mechanics approach with a multiconfigurational and perturbative description of the wave function was employed to compute the minimum, transition state, and conical intersection. It was found that the barrier in the potential energy surface to access the conical intersection funnel increases in aqueous environment, making the system prone to enlarge the emission yield. These results rationalize the observed enhancement of emission in 2-aminopurine upon increasing of the solvent polarity.

© 2008 Elsevier B.V. All rights reserved.

1. Introduction

In modern photophysics, the high photostability with respect to UV light interaction in organic molecules is explained by rapid internal conversion of the absorbed energy due to the presence of accessible funnels of energy degeneration between the excited and the initial ground state. Due to its role in the mechanisms underlying DNA photodamage [1], the nucleobases have been the focus of most attention. Recently, important information on the nucleobases photostability has been obtained by time-resolved fluorescence [2,3] and transient absorption [4,5] spectroscopies. In this context, it has been established that their lowest excited state presents extremely short lifetimes, a phenomenon that can be explained by the ultrafast internal conversion taking place in the picosecond and sub-picosecond time scale after the absorption of light and, consequently, yielding a weak fluorescence emission. The obtained low fluorescence quantum yields are a consequence of the short lifetimes of the spectroscopic excited singlet states. A femtosecond time resolution is therefore required to study the structure and dynamics of DNA [1].

Local variations in the structure of DNA can play important roles in mediating protein-DNA interactions involved in many cellular processes. The characterization of such localized changes requires the use of spectroscopic methods in which a fluorescent probe, obviously different from the weakly emissive natural nucleobases,

is incorporated into DNA at a specific site [6]. Among the most widely probes employed is 2-aminopurine, a constitutional isomer of adenine (see Fig. 1). 2-Aminopurine has good qualities as a probe: the structure of DNA is minimally perturbed by the replacement of adenine by 2-aminopurine, and the latter has high fluorescence quantum yield in contrast with the natural nucleic acid bases. Strong fluorescence in a molecule is typically related with a poor photostability, because it implies that the excited state lifetime is large enough to yield emission, and therefore the molecule is prone to undergo reactivity in its excited state. The modern description of the photochemistry of DNA nucleobases is based on recent works that explain the efficiency of radiationless decay between different electronic states by crossings of different potential energy hypersurfaces (PEH), named conical intersections (CI) [7]. These crossings behave as energy funnels where the probability for non-adiabatic, non-radiative jumps, that is, efficient internal conversion processes, is high [8,9]. Therefore, fluorescence quantum yields and excited lifetimes can be related to the nature of the paths and the barriers that the system has to surmount to reach the crossing seam. The distinct photochemical behavior of the non-natural nucleobase 2-aminopurine (a highly emissive source) and its natural isomer adenine (displaying a very low emissive yield) has been clearly explained by Serrano-Andrés et al. [10] in terms of minimum energy paths, reaction barriers, and accessibility of significant conical intersections. Whereas adenine was shown to display a barrierless energy reaction path along its spectroscopic $\pi\pi^*$ state toward an accessible conical intersection connecting the excited and ground (gs) states, and enabling an efficient, ultrafast non-radiative decay,

* Corresponding author. Fax: +55 67 3345 7190.
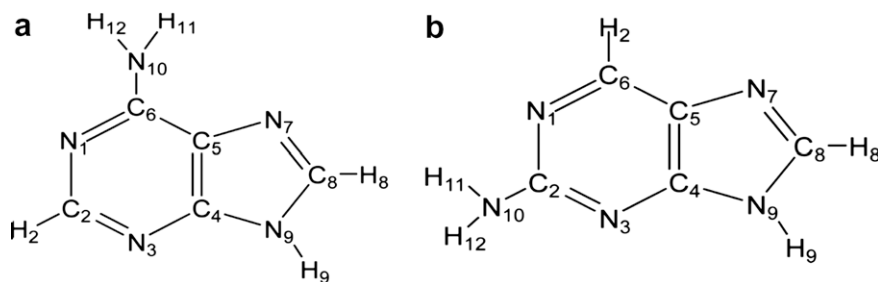E-mail address: ludwig.valdemir@gmail.com (V. Ludwig).

Fig. 1. Structure of (a) adenine (6-aminopurine) and (b) 2-aminopurine.

the equivalent path for 2-aminopurine contained an energy barrier hindering the access to the CI, and consequently increasing the excited state lifetime and leading to emission.

Both adenine and 2-aminopurine can be therefore considered a solid paradigm in favor of the conical intersection concept in modern photochemistry [10], ruling out previous models related with the coupling of higher-lying $n\pi^*$ excited states (such as the so-called proximity effect) [10]. Despite the successful rationalization performed for the isolated system, a full comparison with experiment requires consideration of solvent effects. The environment plays a significant role in the emissive properties of 2-aminopurine. For example, its fluorescence yield increases dramatically as the solvent polarity increases. For its close 9-ethyl-2-aminopurine derivative the quantum yield varies from 0.01 in the non-polar solvent cyclohexane to 0.68 in water [11]. Such type of behavior is at odds with that in adenine, that remains photostable also in solution [1]. If we could understand the photochemical behavior of 2-aminopurine in polar solvents in terms of accessibility of the CIs, the proposed model for internal conversion in DNA nucleobases would be finally consolidated. On the theoretical side an extensive work has been dedicated to the study of the relaxation paths of the nucleic acids bases in the gas phase [7,10,12–18]. Compared with the research activities for isolated molecules, theoretical studies on radiationless decay processes of solvated systems are still limited [19–21]. Some of these studies use a continuum approach for the inclusion of the solvent effects [19,20]. However, it has been clearly established that the specific solute–solvent interaction largely affects the relative energy and properties of the electronic excited states [22].

In order to understand the distinct relaxation and emission properties of 2-aminopurine, we have used the sequential Monte Carlo quantum mechanics (S-MC/QM) approach in which the hydrated environment is modeled by the inclusion of different shells of water molecules mimicked by a distribution of point charges. Statistically uncorrelated solute–solvent configurations are first generated for the subsequent quantum mechanics calculations. As a strategy we have employed the different points belonging to the minimum energy path (MEP) computed at the CASPT2//CASSCF level of theory for the isolated system in its initially populated $\pi\pi^*$ (L_a) excited state [10] and at each of such geometries the solvation has been simulated as described.

2. Methodology

2.1. Electronic structure calculations

As mentioned above, the geometrical configurations obtained as belonging the $\pi\pi^*$ L_a MEP of 2-aminopurine were taken from a previous study on the isolated system [10]. In short, the structures were obtained at the CASSCF level and correspond to points of a connected reaction path computed in a steepest descendent direction. Each step requires the minimization of the PEHs on a hyperspherical cross section of the PEH centered at the initial geometry and characterized by a predefined radius. To study the most important characteristics of the photophysics of 2-aminopurine, we selected geometries at the minima of the ground, $(gs)_{MIN}$, and $\pi\pi^*$ L_a singlet excited state, $(\pi\pi^*)_{MIN}$, the conical intersection relating the ground and lowest energy $\pi\pi^*$ singlet excited state, $(gs/\pi\pi^*)_{CI}$, and the transition state (TS), $(\pi\pi^*)_{TS}$, connecting both excited state points. At the selected points, CASPT2 calculations were carried out to include the necessary dynamic correlation effects. The 6-31G(d,p) one-electron atomic basis sets were used for computing the geometrical configurations and energy differences. The active space includes a total of 16 electrons distributed in 13 orbitals, which is labeled as CAS(16/13); the same active space was employed for the CASPT2 step. As shown before [10], this active space is large enough to include al the $\pi\pi^*$ and $n\pi^*$ states in order to obtain a balanced description of the PEH. The quantum mechanics calculations were performed with the MOLCAS-6 quantum chemistry software [23].

2.2. Solvent effects

The solvent effects for each geometrical configuration were included using the S-MC/QM procedure [24–26]. Standard MC simulations [27] were employed including the Metropolis [28] sampling technique and periodic boundary conditions using the minimum image method in a cubic box, in the canonical NPT ensemble, at room temperature (T = 298 K). Periodic boundary conditions and a cut-off radius of 18.7 Å from the center of mass were used to truncate the sphere of intermolecular separation and long-range corrections beyond this cut-off distance. All simulations were performed using the DICE programs [29].

Intermolecular interactions were modeled by the standard Lennard–Jones and Coulomb potential with three parameters for each interacting site. The water molecules were described by the simple point charge (SPC) potential [30]. The 2-aminopurine (solute) was described by the optimized parameter for liquid simulation (OPLS) parameters [31,32] in the optimized geometry. Single-point CASSCF/6-31G(d,p) calculations and the CHELPG [33] method were used to fit the charges for the 2-aminopurine geometries at the lowest $\pi\pi^*$ state. The total dipole moments calculated for the minimum, transition state and conical intersection (gs/$\pi\pi^*$)$_{CI}$ points are 3.98, 3.59 and 4.20 D, respectively.

By considering the position and orientation of each molecule, the initial configuration is generated randomly. Then, by translating in all cartesian directions and rotating around a randomly chosen axis a new configuration is obtained. The simulations consist of a thermalization phase of 1.8×10^7 MC steps, followed by an average stage of 2×10^8 MC steps, corresponding to 2×10^5 MC steps per molecule. The S-MC/QM procedure was used to analyze the electronic structure of 2-aminopurine in liquid water. The great advantage of this approach is that it reveals the most important MC statistical information, obtained from the autocorrelation function of the energy, before the QM calculation steps, thus reducing significantly the number of supermolecular structures that will be employed in the QM steps. In the present work, configurations

were generated with less than 15% of statistical correlation. A total of 100 configurations were then selected that are apart from one another by 2×10^6 MC steps. The absorption spectra and dipole moments were simulated from the results of a simple average over the QM results for the 100 statistically uncorrelated supermolecular configurations, with the excitation energies computed with the CASPT2 method. In the quantum-chemical calculations, the 2-aminopurine is surrounded by 400 water molecules corresponding to all solvent molecules with a distance of 14.3 Å from the solute (see Fig. 2). The total number of hydrogen bonds provide some useful information on the solute–solvent interaction. Our analysis based on the radial distribution function, indicates that in the lowest $\pi\pi^*$ state there are 0.81, 0.94 and 0.86 water molecules that are hydrogen-bonded to the configuration of the minimum, transition state and conical intersection, respectively. This number is relatively small, around one hydrogen bond. But moving from the minimum of the path to the transition state there is a slight increase in the number of hydrogen bonds in the N3 site and a decrease in the N7 atomic site in the conical intersection. Overall the total number of hydrogen bonds is largest in the transition state and lowest in the minimum.

In the QM calculations, the solvent molecules are represented by the SPC point charges placed at the atomic sites and all the 100 selected configurations were averaged to one configuration, as implemented in the average solvent electrostatic configuration (ASEC) method [34].

3. Results and discussion

Before discussing the solvent effects on the lowest $\pi\pi^*$ state, we will comment on the results for the vertical absorption spectra of isolated 2-aminopurine. The lowest singlet excited states are computed at 4.33, 4.46, and 5.33 eV at the CASPT2 level of calculation. These results are assigned to the $\pi\pi^*$ (L_a), $n\pi^*$, and $\pi\pi^*$ (L_b) transitions, respectively. Compared with previous CASPT2 results obtained with a much larger ANO-L basis set, 4.07, 4.60, and 5.02 eV for the same order of transitions [35], we can see that the present results slightly overestimate the $\pi\pi^*$ transitions and underestimate the $n\pi^*$ transition. Experimentally, no absorption peaks in gas phase have been reported. Pal et al. [2] identified a 0–0 band at 4.01 eV in jet-cooled experiments. Additionally an absorption band maximum was recorded at 4.1 eV for 2-aminopurine in poly(vinyl alcohol)films [36] and in water [37]. Based on these results we conclude that the lowest vertical absorption transition in the gas phase must be located in a range of energies 4.1–4.3 eV.

To understand the energy deactivation and the high emissive quantum yield in polar solutions, we have computed the MEP along the $\pi\pi^*$ (L_a) hypersurface in aqueous solution. As it was shown in a previous study [10] the lowest $\pi\pi^*$ state is directly populated and most of the energy evolves toward a minimum in the $\pi\pi^*$ state PEH. Our present results for gas phase and solvent are presented in Table 1 and Fig. 3. The energy barrier obtained at the CASPT2(16/13) level in gas phase has a value of 2.4 kcal/mol. This result is slightly smaller, but similar, as compared to the 5.0 kcal obtained at the CASPT2(12/11) level of theory. In solution, whereas the pathway remains barrierless toward the state minimum, an increase of the energy barrier from the minimum to the TS is obtained. In the aqueous environment the system has to surmount a barrier of 5.5 kcal/mol to reach the CI, what represents an increase of 3.1 kcal/mol with respect to the gas phase situation. In solution the computed CI stills represents a closely degenerated
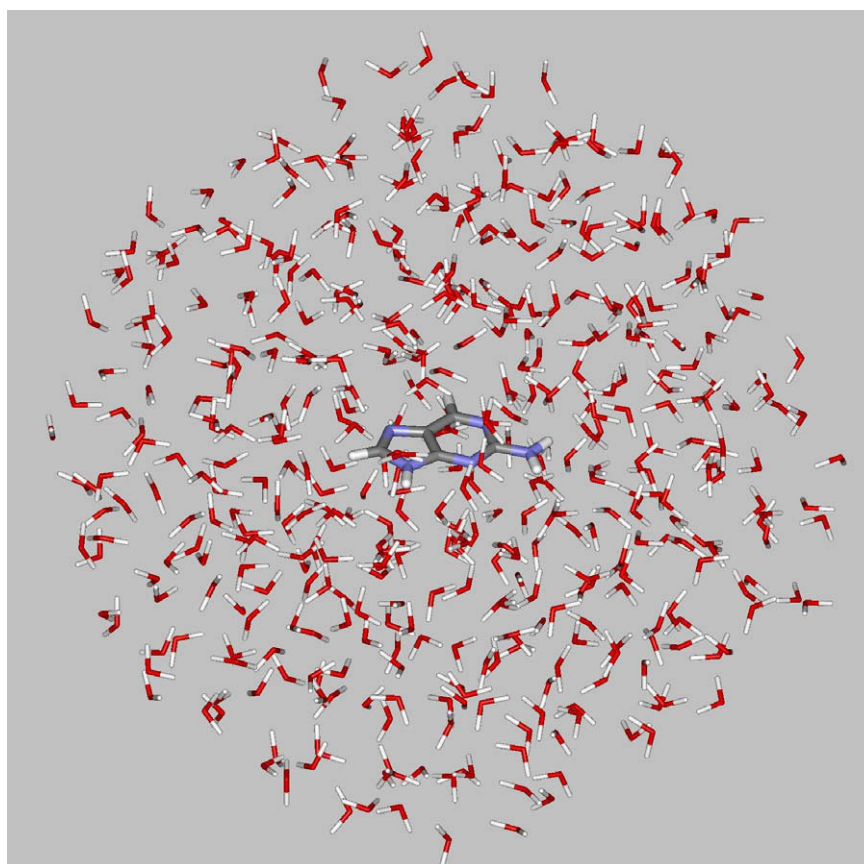

Fig. 2. One supermolecular structure generated by the simulation corresponding to one 2-aminopurine molecules (center) and 400 water molecules.

Table 1
Computed energy barriers (kcal/mol), in gas phase and aqueous solution, for the low-lying singlet excited state of 2-aminopurine at the CASPT2//CASSCF(16/13)/6-31G(d,p) level

Structures	Description	E (water)	E (gas phase)
$(gs/\pi\pi^*)_{CI} - (gs)_{MIN}$	Ground state with respect to the conical intersection point	63.7	72.4
$(gs/\pi\pi^*)_{CI} - (\pi\pi^*)_{TS}$	$\pi\pi^*$ Transition state with respect to the conical intersection point	−16.6	−6.14
$(gs/\pi\pi^*)_{CI} - (\pi\pi^*)_{MIN}$	$\pi\pi^*$ Minima with respect to the conical intersection point	−11.1	−3.7
$(\pi\pi^*)_{TS} - (\pi\pi^*)_{MIN}$	$\pi\pi^*$ Transition state with respect to the minimum of $\pi\pi^*$	5.5	2.4

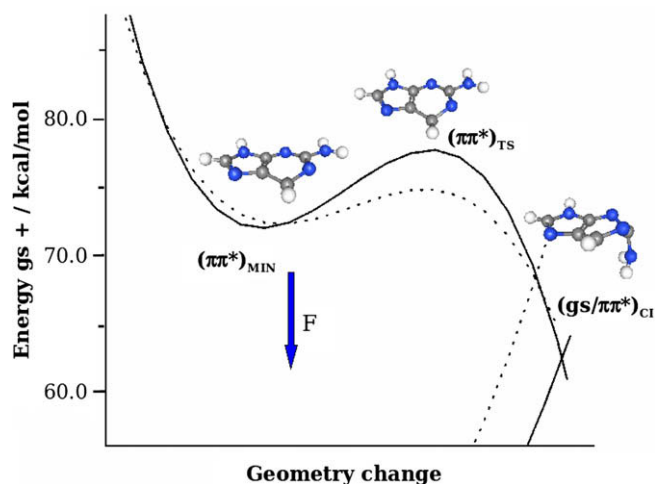Ground state energy = −466.063624 a.u.

Fig. 3. Scheme based on CASPT2 calculations for the lowest $\pi\pi^*$ decay pathway of 2-aminopurine. The dotted line represents the gas phase energy surface and the solid line the aqueous solvent results. The energy of the ground state is −466.063624 a.u. and all the points above given in kcal/mol with respect to the ground state.

situation. The effect of the polar solvent is therefore to stabilize much more the $\pi\pi^*$ state planar minimum that the transition state (TS) and the conical intersection structures, displaying both an out-of-plane ring puckered geometry [10], finally leading to a net increase of the access barrier. This is consistent with the relative values of dipole moments of the states described in Section 2.2. A slightly lower dipole moment of the transition state with respect to the minimum causes its relative destabilization in its interaction with the solvent, enhancing the energy barrier. With respect to the fluorescence band origin, our calculations predict a small red-shift of 1.3 kcal/mol from gas phase to an aqueous environment.

The present combined multiconfigurational quantum-chemical Monte Carlo quantum mechanics calculations represents an efficient approach that can be realistically applied to account for the electronic structure description of the photochemistry of systems of the size of 2-aminopurine. Calculation of MEPs, minima, TS, and accessible CIs enables the calculation of relevant energy barriers both in gas phase and in solution. The key feature of the photophysics of 2-aminopurine in different media has been therefore rationalized just by considering the main spectroscopic $\pi\pi^*$ state and the accessibility of its crossing seam with the ground state, making the claim for the participation of the $n\pi^*$ state unnecessary. Even if such state has been computed at low energies both in adenine and 2-aminopurine [10], its interaction can hardly affect to the main internal conversion process, because its relaxation path belongs to a totally different region of the PEH. In this sense, small

energy gaps may be of limited importance if the interaction region does not match.

4. Conclusions

The aqueous solvent polarization on the lowest-lying $\pi\pi^*$ potential energy surface of 2-aminopurine was studied theoretically using a sequential Monte Carlo quantum mechanics model, based on statistically uncorrelated configurations and a multiconfigurational and perturbative description of the wave function by means of the CASSCF and CASPT2 methods. These results are the first quantitative and accurate estimate of the accessibility of a conical intersection seam of 2-aminopurine in solvated phases using a robust solvation model, reinforcing the reliability of our combined approach for quantitative predictions.

Based on carefully computed minimum energy paths for the lowest excited singlet excited state, an increase of 3.1 kcal/mol in the energy barrier of the $\pi\pi^*$ state to access the conical intersection with the ground state was obtained with respect to the value for the isolated system. This result is in line with experimental measurements of the increase of fluorescence emission of 2-aminopurine in polar solvents.

According to the schematic view yielded by the calculations for 2-aminopurine, the increase of the barrier in water will reduce the non-radiative yield, increasing the emission and the excited state lifetime. In the gas phase a large fraction of the initially absorbed energy will be able to overcome the reaction barrier and decay non-radiatively to the ground state, leading to a low fluorescence quantum yield. Those findings are in agreement with the trends observed for 2-aminopurine and its close derivative 9-ethyl-2-aminopurine, which displays a fluorescence quantum yield of 0.01 in the non-polar solvents that increases to 0.68 in water [11].

References

[1] C.E. Crespo-Hernández, B. Cohen, P.M. Hare, B. Kohler, Chem. Rev. 104 (2004) 1977.
[2] S.K. Pal, J. Peon, A.H. Zewail, Chem. Phys. Lett. 363 (2002) 57.
[3] T. Gustavsson, A. Sharanow, D. Onidas, D. Markovitsi, Chem. Phys. Lett. 356 (2002) 49.
[4] C. Canuel, M. Mons, F. Piuzzi, B. Tardivel, I. Dimicoli, M. Elhamin, J. Chem. Phys. 122 (2005) 074316.
[5] B. Cohen, P.M. Hare, B. Kohler, J. Am. Chem. Soc. 125 (2003) 13594.
[6] E.L. Rachofsky, R. Osman, J.B.A. Ross, Biochemistry 40 (2001) 946.
[7] L. Serrano-Andrés, M. Merchán, A.C. Borin, J. Am. Chem. Soc. 108 (2008) 2473, and references therein.
[8] M. Klessinger, J. Michl, Excited States and Photochemistry of Organic Molecules, VCH, New York, 1995.
[9] M. Olivucci (Ed.), Computational Photochemistry, Elsevier, Amsterdam, 2005.
[10] L. Serrano-Andrés, M. Merchán, A.C. Borin, Proc. Natl. Acad. Sci. USA 103 (2006) 8691.
[11] D.C. Ward, E. Reich, L. Stryer, J. Biol. Chem. 244 (1969) 1228.
[12] S. Perun, A.L. Sobolewski, W. Domcke, J. Am. Chem. Soc. 127 (2005) 6257.
[13] L. Serrano-Andrés, M. Merchán, A.C. Borin, Chem. Eur. J. 12 (2006) 6559.
[14] M. Merchán, L. Serrano-Andrés, M.A. Robb, L. Blancafort, J. Am. Chem. Soc. 127 (2005) 1820.
[15] S. Matsika, J. Phys. Chem. A 108 (2004) 7584.
[16] H. Chen, S. Li, J. Chem. Phys. 124 (2006) 154315.
[17] C.M. Marian, J. Chem. Phys. 122 (2005) 104314.
[18] M. Barbatti, A.J.A. Aquino, H. Lischka, J. Phys. Chem. A 109 (2005) 5168.
[19] B. Mennucci, A. Toniolo, J. Tomasi, J. Phys. Chem. A 105 (2001) 4749.

[20] T. Gustavsson, N. Sarkar, E. Lazarotto, D. Markovitsi, V. Barone, R. Importa, J. Phys. Chem. B 110 (2006) 12843.
[21] S. Yamazaki, S. Kato, J. Am. Chem. Soc. 129 (2007) 2901.
[22] V. Ludwig, K. Coutinho, S. Canuto, Phys. Chem. Chem. Phys. 9 (2007) 1.
[23] G. Karlström et al., Comput. Mater. Sci. 28 (2003) 222.
[24] S. Canuto, K. Coutinho, Adv. Quantum Chem. 28 (1997) 89.
[25] K. Coutinho, S. Canuto, J. Chem. Phys. 113 (2000) 9132.
[26] K. Coutinho, S. Canuto, M.C. Zerner, J. Chem. Phys. 112 (2000) 9874.
[27] M.P. Allen, J.D. Tildesley, Computer Simulation of Liquids, Oxford University Press, Oxford, UK, 1987.
[28] N. Metropolis, A.W. Rosenbluth, M.N. Rosenbluth, A.H. Teller, E. Teller, J. Chem. Phys. 21 (1953) 1087.
[29] K. Coutinho, S. Canuto, A Monte Carlo Program for Molecular Liquid Simulation, University of São Paulo, São Paulo, SP, Brazil, 2000.
[30] H.J.C. Berendsen, J.P.M. Postma, W.F. van Gunsteren, B. Pullman (Eds.), Intermolecular Forces, Reidel, Dordrecht, The Netherlands, 1981.
[31] W.L. Jorgensen, J.M. Briggs, M.L. Contreras, J. Phys. Chem. 94 (1990) 1683.
[32] W.L. Jorgensen, D.L. Severance, J. Am. Chem. Soc. 112 (1990) 4768.
[33] C.M. Breneman, K.B. Wiberg, J. Comput. Chem. 11 (1990) 361.
[34] K. Coutinho, H.C. Georg, T. Fonseca, V. Ludwig, S. Canuto, Chem. Phys. Lett. 437 (2007) 148.
[35] A.C. Borin, L. Serrano-Andrés, V. Ludwig, K. Coutinho, S. Canuto, Int. J. Quantum Chem. 106 (2006) 2564.
[36] A. Holmen, B. Nordén, B. Albinsson, J. Am. Chem. Soc. 119 (1997) 3114.
[37] C. Santhosh, P.C. Mishra, Spectrochim. Acta 47 (1991) 1685.